Author(s): Struch, Niklas; Topic, Filip; Rissanen, Kari; Lützen, Arne

Title: Electron-deficient trifluoromethyl-substituted sub-components affect the properties of M4L4 tetrahedral cages

Year: 2017

Version:

Please cite the original version:

Struch, N., Topic, F., Rissanen, K., & Lützen, A. (2017). Electron-deficient trifluoromethyl-substituted sub-components affect the properties of M4L4 tetrahedral cages. Dalton Transactions, 46(33), 10809-10813. https://doi.org/10.1039/C7DT02182H

Dalton Transactions

Accepted Manuscript

This article can be cited before page numbers have been issued, to do this please use: N. Struch, F. Topi, K. Rissanen and A. Lützen, *Dalton Trans.*, 2017, DOI: 10.1039/C7DT02182H.

ROYAL SOCIETY OF CHEMISTRY

rsc.li/dalton

View Article Online
DOI: 10.1039/C7DT02182H

Journal Name

ARTICLE

Electron-deficient trifluoromethyl-substituted sub-components affect the properties of M_4L_4 tetrahedral cages

Received 00th January 20xx,
Accepted 00th January 20xx

DOI: 10.1039/x0xx00000x

www.rsc.org/

N. Struch,[a] F. Topić,[b] K. Rissanen,[b] and A. Lützen[a]

Two supramolecular tetrahedral cages based on a new electron-deficient trifluoromethyl-substituted pyridylimine ligand are synthesised by sub-component self-assembly. Their structures are characterised by NMR und UV-Vis spectroscopy, high-resolution mass spectrometry and single crystal X-ray diffraction and show host-guest chemistry, complex-to-complex transformations and novel electronic properties.

Introduction

The implementation of functionality into supramolecular aggregates is one of the major challenges in modern metallo-supramolecular chemistry.[1] This may include novel functional ligands,[2] utilising cavities and voids[3] in the aggregates or utilising the properties of the metal centres themselves.[4]
Complex-to-complex transformations with varying ligand systems are also a field of major interest, allowing the use of the properties of one ligand and subsequent utilization of the second ligand.[5] Possible applications of this procedure have been shown for structurally similar but "inverted" ligand systems.[‡,6] Here, the electronic effects of the ligands play a major role both in supramolecular chemistry in general as well as other fields of interest, for example the field of spin-crossover research.[7]
Hence, we focused on investigating the properties of new ligand systems in order to both adjust the binding properties of the new ligands to metal centres like iron(II) and generate new supramolecular structures.

Results and discussion

Cages **1** and **2** were synthesized in a sub-component self-assembly process (Scheme 1). A degassed mixture of 4 equivalents of pararosaniline base, 12 equivalents of 5-trifluoromethylpyridyl-2- carbaldehyde and 4 equivalents of iron(II) triflimide hydrate for 1 or zinc(II) triflimide hydrate for

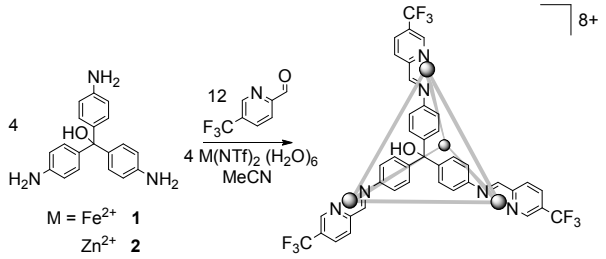

Scheme1. Synthesis of cages **1** and **2**.

2, respectively) in acetonitrile was heated at 70 °C for 18 hours. A quick workup procedure of precipitating the product by addition of excess diethyl ether, filtration, washing with dichloromethane and generous amounts of diethyl ether and drying in a stream of air yielded the products in typical yields of 85%.
As shown by ^{1}H- (Figure 1) and ^{13}C-NMR spectra (SI) the structures of both cages **1** and **2** are highly symmetric, comprising a single set of signals in accordance with the structure shown in scheme **1**. The UV-Vis spectra (SI) of both **1** and **2** contain the bands associated with the pararosaniline chromophore backbone (shifted by the included imine moieties and the coordinated metal centres) and the metal-N_6-chromophores.[8]

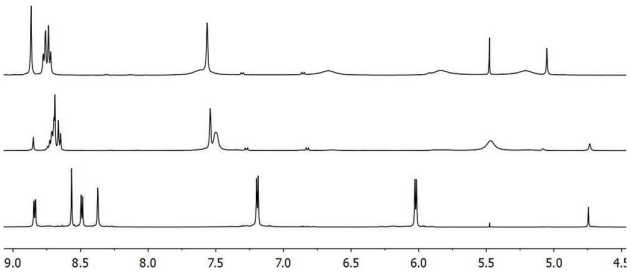

Figure 1. Excerpt from the ^{1}H-NMR spectra of **1** (top), NO_3^-**@1** (middle) and **2** (bottom), acetonitrile-*d3*, 298 K.

[a] *Kekulé Institut für Organische Chemie und Biochemie*
Rheinische Friedrich-Wilhelms-Universität Bonn
Gerhard-Domagk-Straße 1
53121 Bonn, Germany
E-mail: arne.luetzen@uni-bonn.de.
[b] *University of Jyväskylä*
Department of Chemistry, Nanoscience Center
P.O. Box 35, 40014 Jyväskyla, Finland.
Electronic Supplementary Information (ESI) available: Experimental procedures, NMR spectra, mass spectra, IR spectra, UV/Vis spectra, additional grafics, tables of single crystal XRD data. CCDC 1540569. See DOI: 10.1039/x0xx00000x

View Article Online
DOI: 10.1039/C7DT02182H

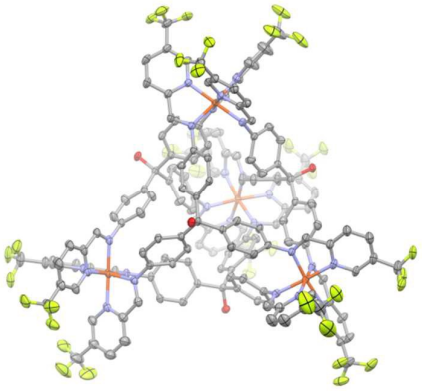

Figure 2. The X-ray structure of the cationic unit of **1**. Thermal ellipsoids are shown at 30% probability level. Colour code: Grey – carbon, blue – nitrogen, red – oxygen, yellow – fluorine. Hydrogen atoms are omitted for clarity.

Furthermore, its (supra-)molecular composition was proven by high-resolution mass spectrometry (SI). Finally, the crystal structure of the mixed hexafluorophosphate (PF_6^-) and triflate ($CF_3SO_3^-$) salt of **1** was obtained. Crystals were grown from a solution of **1** with triflate as the counter-anion and an excess of KPF_6 in a mixture of acetonitrile and chloroform by gas diffusion of diisopropyl ether. The cage **1** was found to crystallise in the space group *I*2/*a* with one half of the cage in the asymmetric unit. Iron(II) metal centres exhibit the low-spin configuration, with Fe-N bond lengths between 1.966(3) and 1.986(3).

The cage was found to possess an internal cavity with a volume of 42 Å^3, just big enough to accommodate a nitrate (NO_3^-) anion. Indeed, addition of 1.2 equivalents of KNO_3 to a solution of cage **1** in acetonitrile and heating to 60°C for 1 hour resulted in the host-guest complex NO_3^-@**1** in nearly quantitative yield. Addition of one equivalent of nitrate per cage **1** and equilibrating the system for one hour yielded a mixture of empty and filled cages.[9] From this experiment we could deduce a binding constant of $K = 10.8 \pm 1.9 \cdot 10^3$ M^{-1} ($\log(K)=4.03 \pm 0.08$). This is of the same order of magnitude as found for other, structurally similar cages.[10] While the parent structure reportedly does not bind any guests the slight change in electronic properties and the added equilibration step might be the key for enabling the binding of small anions.

While the slightly longer Zn-N bond length, hailing from the d^{10} configuration of Zn, allows for the free rotation of aryl spacers in **2** already at room temperature, the free rotation of aryl spacers in **1** is only possible at temperatures above 313 K (SI), due to the low-spin d^6 configuration of its Fe(II) centres .

As expected for an electron-deficient pyridylimine derivative, some properties differ from those of the parent pyridylimine structure.[9] Most notably, this is a slightly different ligand field splitting at the metal centres which, while mostly irrelevant for the closed-shell d^{10}-configured zinc(II) centres, has a notable impact on the properties of the iron(II) centres. Shifted $^1A_{1g} \rightarrow {}^5T_{2g}$ transitions in the UV-Vis spectra (from 566 nm in the parent structure[8] to 580 nm in **1**) are observed.

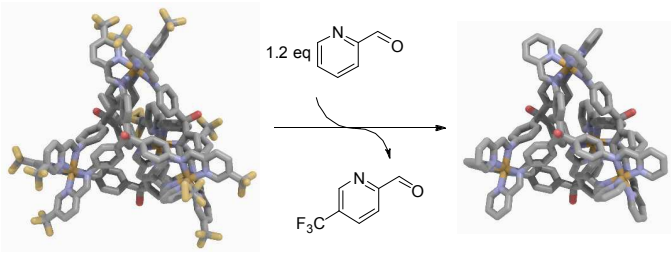

Figure 3. Complex-to-complex transformation of **1** to the parent structure.[9]

The reduced electron density in the pyridyl system and, hence, the reduced σ-donating character of the nitrogen lone pair results in a slightly reduced ligand field splitting (see the SI).[7] Accordingly, a slight stabilisation of the $^5T_{2g}$ high-spin state compared to the $^1A_{1g}$ low-spin ground state can be observed by temperature-dependent NMR experiments, resulting in a slight population of the high-spin state at room temperature and above leading to temperature-dependent increased shifts in NMR spectra.[11]

Another interesting feature of systems involving electron-deficient ligands is the altered stability of the formed complexes. While the aggregates are stable in solution and gas phase, complex-to-complex transformations of the system can still be observed. By addition of more electron-rich ligand fragments (like e.g. pyridyl-2-carbaldehyde in a slight excess) **1** can be fully converted to the more stable parent structure (Figure 3).

Conclusions

In summary, we have synthesised and characterised two novel supramolecular tetrahedral Fe(II) and Zn(II)-based cages possessing a trifluoromethyl-substituted pyridylcarbaldehyde fragment. The tetranuclear iron(II) cage can encapsulate small anionic guests such as nitrate in its inner cavity. It furthermore exhibits novel properties such as e.g. a slight stabilization of paramagnetic $^5T_{2g}$ excited states as well as offering the possibility of complex-to-complex transformation which has not been established for aniline-backbone structures before. The presented systems were characterised by means of different NMR spectroscopic techniques, UV-Vis spectroscopy, high-resolution mass spectrometry and IR spectroscopy. Furthermore, **1** was also characterised by single crystal X-ray diffraction.

Experimental

General remarks

All substances were purchased from Alfa Aesar, J.T. Baker, Sigma-Aldrich or VWR Chemicals and used without further purification. 5-(Trifluoromethyl)-pyridyl-2-carbaldehyde was purchased from Fluorochem and used without further purification. NMR spectra were recorded on a Bruker Advance DPX 700, DPX 500 or DPX 300. Chemical shifts δ are given in

View Article Online
DOI: 10.1039/C7DT02182H

ppm relative to residual solvent signals (^{1}H).[12] For labelling schemes of the individual nuclei of metallosupramolecular cages **1** and **2** see SI. ESI mass spectra were recorded on a Fischer Scientific LTQ Orbitrap XL. FT-IR spectra were recorded on a Thermo Nicolet 380 FT-IR. UV-Vis spectra were recorded on a Jena Analytic Specord 200 spectrometer using a 10 mm cuvette.

Synthesis and characterisation of 1

A solution of 15 mg pararosaniline base (0.05 mmol, 4 eq), 25 mg 5-(trifluoromethyl)-pyridyl-2-carbaldehyde (0.15 mmol, 12 eq) and 37 mg iron(II) triflimide hexahydrate (0.5 mmol, 4 eq) in 2 mL acetonitrile (HPLC grade) were degassed by one freeze-pump-thaw cycle and flushed with argon and heated to 65 °C for 18 hours. After cooling the solution to room temperature the solution was poured in 20 mL diethyl ether, the precipitate was filtered off, washed with dichloromethane and generous amounts of diethyl ether and dried in a stream of air to yield 59 mg (0.01 mmol, 85 %) purple-pink powder.
^{1}H-NMR (acetonitrile-*d3*, 298 K, 500.1 MHz, δ in ppm) = 8.84 (s, 3H, H4), 8.74 (d, $^3J_{H3H2}$=8.7 Hz, 3H, H3), 8.70 (d, $^3J_{H2H3}$=8.7 Hz, 3H, H2), 7.59 (brs, 3H, H5/6*), 7.54 (s, 3H, H1), 6.65 (brs, 3H, H5/6*), 5.81 (brs, 3H, H5/6*), 5.81(brs, 3H, H5/6*), 5.02 (s, 1H, H7) (*due to the broad nature of the signals no significant cross-peaks can be observed in the 2D spectra); ^{13}C-NMR (acetonitrile-*d3*, 298 K, 156.4 MHz δ in ppm) = 176.7 (f), 160.4 (b), 153.5 (a), 149.8 (e), 147.6 (j), 140.9 (g), 138.8 (d), 131.7 (c), 130.8 (q, CF3), 123.0 (h/i*), 121.1 (h/i*), 120.8 (h/i*), 118.6 (h/i*), 80.5 (k) (*due to the broad nature of the signals no significant cross-peaks can be observed in the 2D spectra); ^{19}F-NMR (acetonitrile-*d3*, 298 K, 282.4 MHz, δ in ppm) = -63.4 (-CF_3), -79.9 (NTf$^-$); high resolution ESI-MS (acetonitrile, positive mode, *m/z*) = 515.6343 (calcd. for $(C_{40}H_{25}F_9N_6O)_4Fe_4(NS_2O_4C_2F_6)]^{7+}$ 515,6341), 648.2262 (calcd. for $[C_{40}H_{25}F_9N_6O)_4Fe_4(NS_2O_4C_2F_6)_2]^{6+}$ 648,2260), 834.0540 (calcd. for $[C_{40}H_{25}F_9N_6O)_4Fe_4(NS_2O_4C_2F_6)_3]^{5+}$ 834.0546); UV-Vis (acetonitrile, 298 K, λ in nm) = 234, 282, 326, 538, 580.

Synthesis and characterisation of 2

A solution of 15 mg pararosaniline base (0.05 mmol, 4 eq), 25 mg 5-(trifluoromethyl)-pyridyl-2-carbaldehyde (0.15 mmol, 12 eq) and 37 mg zinc(II) triflimide hexahydrate (0.5 mmol, 4 eq) in 2 mL acetonitrile (HPLC grade) was degassed by one freeze-pump-thaw cycle and flushed with argon and heated to 65 °C for 18 hours. After cooling the solution to room temperature the solution was poured in 20 mL diethyl ether, the precipitate was filtered off, washed with dichloromethane and generous amounts of diethyl ether and dried in a stream of air to yield 61 mg (0.01 mmol, 86%) bright pink powder.
^{1}H-NMR (acetonitrile-*d3*, 298 K, 700.1 MHz, δ in ppm) = 8.81 (dd, $^3J_{H3H2}$=8.2 Hz, $^5J_{H3H1}$=1.6 Hz, 3H, H3), 8.54 (s, 3H, H4), 8.46 (d, $^3J_{H2H3}$=8.2 Hz, 3H, H2), 8.34 (brs, 3H, H1), 7.16 (d, $^3J_{H5H6}$=8.4 Hz, 6H, H5), 5.99 (d, $^3J_{H6H5}$=8.4 Hz, 6H, H6), 4.71 (s, 3H, H7); ^{13}C-NMR (acetonitrile-*d3*, 298 K, 156.4 MHz δ in ppm) = 165.7 (f), 148.9 (b), 147.3 (a), 146.7 (g), 146.6 (j), 141.3 (d), 131.7 (q, -CF_3), 131.3 (c), 128.7 (i), 123.0 (h), 120.6 (e), 80.7 (k); ^{19}F-NMR (acetonitrile-*d3*, 298 K, 282.4 MHz δ in ppm) = -63.35 (-CF_3), -80.13 (NTf$^-$); high resolution ESI-MS (acetonitrile, positive mode, *m/z*) = 420.936 (calcd. for $C_{160}H_{100}F_{36}N_{24}O_4Zn_4^{8+}$ 420.936), 521.059 (calcd. for $[(C_{40}H_{25}F_9N_6O)_4Zn_4(NS_2O_4C_2F_6)]^{7+}$ 521.058), 654.554 (calcd. for $[(C_{40}H_{25}F_9N_6O)_4Zn_4(NS_2O_4C_2F_6)2]^{6+}$ 645.576), 841.649 (calcd. for $[(C_{40}H_{25}F_9N_6O)_4Zn_4(NS_2O_4C_2F_6)3]^{5+}$ 841.649), 1122.041 (calcd. for $[(C_{40}H_{25}F_9N_6O)_4Zn_4(NS_2O_4C_2F_6)4]^{4+}$ 1122.040); UV-Vis (acetonitrile, 298 K, λ in nm) = 230, 286, 342, 504, 530.

Transformation from 1 to the parent structure

A solution of 10.0 mg (0.0017 mmol, 1 eq) **1** and 2.5 mg (0.023 mmol, 13.2 eq) pyridyl-2-carbaldehyde in 0.6 mL acetonitrile-*d3* was heated to 50 °C for 18 hours. The resulting mixture was analysed by NMR-spectroscopy. Afterwards the solution was poured in diethyl ether, filtered, the remaining precipitate was washed with dichloromethane and diethyl ether and dried in a stream of air to yield the pure parent compound in 6 mg (0.0013 mmol, 72%) isolated yield. The resulting 1H-NMR spectrum is in accordance with previously published NMR data.[10]

Synthesis and characterisation of NO_3^-@1

A solution of 10.0 mg (0.0017 mmol, 1 eq) **1** and 0.17 mg (0.0017 mmol, 1.0 eq) KNO_3 in 0.6 mL acetonitrile-*d3* was heated to 60 °C for 2 hours and the resulting solution was analysed by NMR spectroscopy.
^{1}H-NMR (acetonitrile-*d3*, 298 K, 700.1 MHz, δ in ppm) =8.65 – 8.75 (m, 6 H, H2/H3), 8.70 (s, 3 H, H4), 7.53 (s, 3H, H1), 7.50 (brs, 6 H, H5/6*), 5.47 (brs, 6H, H5/6*), 4.76 (s, 1H, H7) (*Due to the braod nature of the peaks no significant cross peaks could be assigned in the 2D spectra); ^{13}C-NMR (acetonitrile-*d3*, 298 K, 156.4 MHz δ in ppm) = 175.5 (f), 160.8 (b), 153.1 (a), 149.2 (e), 147.1 (j), 140.8 (g), 138.4 (d), 130.7 (c), 130.6 (q, CF3), 122.0 (h/i*), 120.7 (h/i*), 120.3 (h/i*), 118.9 (h/i*), 81.1 (k) (*Due to the braod nature of the peaks no significant cross peaks could be assigned in the 2D spectra); ^{19}F-NMR (acetonitrile-*d3*, 298 K, 282.4 MHz, δ in ppm) = -65.4 (-CF_3), -79.9 (NTf$^-$); high resolution ESI-MS (acetonitrile, positive mode, *m/z*) = 484.503 (calcd. for $[NO_3@(C_{40}H_{25}F_9N_6O)_4Fe_4]^{7+}$ 484.501), 575.752 (calcd. for $[NO_3@(C_{40}H_{25}F_9N_6O)_4Fe_4(NO_3)]^{6+}$ 575.582), 703.101 (calcd. for $[NO_3@(C_{40}H_{25}F_9N_6O)_4Fe_4(NO_3)2]^{5+}$ 703.101), 746.687 (calcd. for $[NO_3@(C_{40}H_{25}F_9N_6O)_4Fe_4(NO_3)_1(NS_2O_4C_2F_6)]^{5+}$ 746.685), 790.471 (calcd. for $[NO_3@(C_{40}H_{25}F_9N_6O)_4Fe_4(NS_2O_4C_2F_6)_2]^{5+}$790.469), 1003.586 (calcd. for $[NO_3@(C_{40}H_{25}F_9N_6O)_4Fe_4(NO_3)(NS_2O_4C_2F_6)_2]^{4+}$ 1003.581), 1504.065 (calcd. for $[NO_3@(C_{40}H_{25}F_9N_6O)_4Fe_4(NS_2O_4C_2F_6)_4]^{3+}$ 1504.060), 1058.068 (calcd. for $[NO_3@(C_{40}H_{25}F_9N_6O)_4Fe_4(NO_3)(NS_2O_4C_2F_6)_3]^{4+}$ 1058.065), UV-Vis (acetonitrile, 298 K, λ in nm) = 235, 275, 337, 543, 583.
Due to the procedure without any purification a small amount of free ligand can be observed.

View Article Online
DOI: 10.1039/C7DT02182H

Crystallographic analysis of 1_PF6_TfO

Single crystal X-ray diffraction data were collected on an Agilent SuperNova Dual diffractometer with an Atlas detector using mirror-monochromatized Cu-Kα radiation (λ = 1.54184 Å) from a microfocus source, equipped with an Oxford Cryostream cooling system. CrysAlisPro[13] software was used for data collection, integration and reduction as well as applying the analytical and semi-empirical absorption corrections.

The structures were solved by direct methods using SHELXT-2014/5[14] and refined by full-matrix least-squares using SHELXL-2016/6[15] within the OLEX2[16] and WinGX[17] environment. All non-hydrogen atoms were refined anisotropically. The positions of hydrogen atoms were calculated and refined as riding on the parent carbon atoms with U_H = 1.5 U_C (for methyl groups) or U_H = 1.2 U_C otherwise. PLATON[18] was used for the accurate calculation of geometrical parameters, while the figures were generated using Mercury[19] and QuteMol.[20]

All the ligands' trifluoromethyl ($-CF_3$) groups' geometries were restrained, with all C-F bonds as well as F···F and C···F distances restrained to be equal. Two of the $-CF_3$ groups were also modelled as disordered over two components each, with respective occupancies refining to 0.540(19)/0.460(19) and 0.565(9)/0.435(9).

Out of expected anions, only three anion-occupied positions could be modelled explicitly. One of the positions was modelled as fully occupied by a hexafluorophosphate (PF_6^-) anion, while the next one was modelled as occupied by a PF_6^- anion, disordered over two components with respective occupancies of 0.437(5) and 0.163(5). Finally, the third position was modelled as partially occupied by a triflate ($CF_3SO_3^-$) anion [occupancy 0.365(4)] and a (PF_6^-) anion [occupancy 0.235(4)]. The geometries of PF_6^- anions were restrained to be regular and identical, while the $CF_3SO_3^-$ anion was modelled as a rigid body using the coordinates extracted from a published structure, CSD refcode MEFHOW.[21] Their atomic displacement parameters were also appropriately restrained.

Moreover, three acetonitrile molecules could be located and modelled, one of which with half-occupancy. Their geometries were restrained to be the same, and the rigid-body restraints were applied to their atomic displacement parameters.

Finally, the rest of the solvent molecules were found to be too badly disordered and could not be modelled explicitly. The SQUEEZE[22] routine of PLATON[18,23] was used to calculate the contribution of electron density in these regions to the structure factors in form of FAB files which were used in subsequent refinement cycles.

Crystal dimensions 0.415×0.244×0.190 mm^3, dark violet block, $C_{170.72}H_{111}F_{60.23}Fe_4N_{29}O_{6.17}P_{3.67}S_{0.73}$, M = 4172.09, monoclinic, space group $I2/a$, a = 39.5026(9), b = 21.4950(6), c = 30.4701(9) Å, α = 90, β = 90.077(2), γ = 90°, V = 25872.4(12) Å^3, Z = 4, ρ = 1.071 g cm^{-3}, μ = 2.816 mm^{-1}, F(000) = 8402, 43952 reflections ($2\vartheta_{max}$ = 148.67°) measured (24429 unique, R_{int} = 0.0266, 96.2% completeness at $2\vartheta_{full}$ = 135.50°), Final R indices ($I > 2\sigma(I)$): R_1= 0.0965, wR_2 = 0.2914, R indices (all data): R_1= 0.1138, wR_2 = 0.3161. GOF = 1.283 for 1479 parameters and 2203 restraints, largest diff. peak and hole 2.543/–1.494 eÅ^{-3}. CCDC-1540569 contains the supplementary data for this structure. These data can be obtained free of charge via www.ccdc.cam.ac.uk/data_request/cif, or by emailing data_request@ccdc.cam.ac.uk, or by contacting The Cambridge Crystallographic Data Centre, 12, Union Road, Cambridge CB2 1EZ, UK; fax: +44 1223 336033.

Acknowledgements

Financial support from DFG (SFB 813 – Chemistry at Spin Centers) and the Academy of Finland (K.R.: project no's. 263256, 292746 and 265328) is gratefully acknowledged. N.S. thanks Evonik Foundation for a doctoral scholarship.

Notes and references

‡ Please note: Here, "inverted" means that the structure-forming backbone consists of linked pyridylcarbaldehyde structures and the ligand is formed by the addition of aniline derivatives. See Ref. 11.

1 P. A. Gale, J. W. Steed (eds.), *Supramolecular Chemistry: From Molecules to Nanomaterials*, 2012, John Wiley & Sons, Hoboken.
2 F. Würthner, *Chem. Commun*, 2004, 1564.
3 a) T. S. Koblenz, J. Wassenaar, J. N. H. Reek, *Chem. Soc. Rev.*, 2008, **37**, 247; b) M. Yoshizawa, J. K. Klosterman, M. Fujita, *Angew. Chem. Int. Ed*. 2009, **48**, 3418; c) M. D. Pluth, R. G. Bergman, K. N. Raymond, *Acc. Chem. Res*. 2009, **42**, 1650; d) S. H. A. M. Leenders, R. Gramage-Doria, B. de Bruin, J. N. H. Reek, *Chem. Soc. Rev*. 2015, **44**, 433; e) A. Galan, P. Ballester, *Chem. Soc. Rev*. 2016, **45**, 1720.
4 P. R. Symmers, M. J. Burke, D. P. August, P. I. T. Thomson, G. S. Nichol, M. R. Warren, C. J. Campbell, P. J. Lusby, *Chem. Sci.*, 2015, **6**, 756.
5 Y. R. Hristova, M. M. J. Smulders, J. K. Clegg, B. Breiner, J. R. Nitschke, *Chem. Sci.*, 2011, **2**, 638.
6 C. S. Wood, T. K. Ronson, A. M. Belenguer, J. J. Holstein, J. R. Nitschke, *Nat. Chem.*, 2015, **7**, 354
7 a) R. A. Bilbesi, S. Zarra, H. L. C. Feltham, G. N. L. Jameson, J. C. Klegg, S. Brooker, J. R. Nitschke, *Chem. Eur. J.*, 2013, **25**, 8058; b) A. Ferguson, M. A. Squire, D. Siretanu, D. Mitcov, C. Mathonière, R. Clérac, P. E. Kruger, *Chem. Commun*., 2013, **49**, 1597; c) L. Li, Y. Zhang, D. J. Fanna, N. D. Shepherd, J. K. Clegg, R. Zheng, S. Hayami, L. F. Lindoy, J. R. Aldrich-Wright, C. G. Li, J. K. Reynolds, D. G. Harman, F. Li, *J. Mater. Chem. C*, 2015, **3**, 7878.
8 P. Gütlich, A. Hauser, H. Spiering, *Angew. Chem. Int. Ed.*, 1994, **33**, 2024.
9 The tetranuclear zinc(II) cage **2** decomposes upon exposure to nitrate ions.
10 R. A. Bilbesi, J. K. Clegg, N. Elgrishi, X. de Hatten, M. Devillard, B. Breiner, P. Mal, J. R. Nitschke, *J. Am. Chem. Soc.*, 2012, **134**, 5110.
11 W. C. Isley III, S. Zarra, R. K. Carlson, R. A. Bilbesi, T. K. Ronson, J. R. Nitschke, L. Gagliardi, C. J. Cramer, *Phys. Chem. Chem. Phys.*, 2014, **16**, 10620.
12 G. R. Fulmer, A. J. M. Miller, N. H. Sherden, H. E. Gottlieb, A. Nudelman, B. M. Stoltz, J. E. Bercaw, K. I Goldberg, *Organometallic*s, 2010, **29**, 2176.
13 Rigaku Oxford Diffraction, 2015, CrysAlisPro Software system, version 1.171.38.43, Rigaku Corporation, Oxford, UK.

View Article Online
DOI: 10.1039/C7DT02182H

14 G. M. Sheldrick, *Acta Cryst.* 2015, **A71**, 3.
15 G. M. Sheldrick, *Acta Cryst.* 2015, **C71**, 3.
16 O. V. Dolomanov, L. J. Bourhis, R. J. Gildea, J. A. K. Howard, H. Puschman, *J. Appl. Cryst.* 2009, **42**, 339.
17 L. J. Farrugia, *J. Appl. Cryst.* 2012, **45**, 849.
18 A. L. Spek, *Acta Cryst.* 2009, **D65**, 148.
19 C. F. Macrae, P. R. Eddington, P. McCabe, E. Piddock, G. P. Shields, R. Taylor, M. Towler, J. van de Streek, *J. Appl. Cryst.* 2006, **39**, 453.
20 M. Tarini, P. Cigoni, C. Montani, *IEEE Transactions on Visualization and Computer Graphics* 2006, **12**, 1237.
21 C. R. Groom, F. H. Allen, *Angew. Chem. Int. Ed.* 2014, **53**, 662.
22 A. L. Spek, *Acta Cryst.* 2015, **C71**, 9.
23 A. L. Spek, *J. Appl. Cryst.* 2003, **36**, 7.

TOC graphic

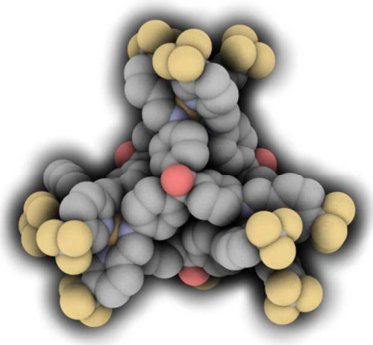

Two supramolecular cages based on a trifluoromethyl-substituted pyridylimine ligand have been synthesised that show host-guest chemistry and complex-to-complex transformations.